*REVISED Manuscript UNMARKED

Click here to view linked References

Marine dual fuel engine modelling and parametric investigation of engine settings effect on performance-emissions trade-offs

Sokratis Stoumpos[a, 1], Gerasimos Theotokatos[a,1], Evangelos Boulougouris[a], Dracos Vassalos[a], Iraklis Lazakis[b], and George Livanos[c]

[a] Maritime Safety Research Centre, Department of Naval Architecture, Ocean and Marine Engineering, University of Strathclyde, 100 Montrose Street, Glasgow, G4 0LZ, Scotland, UK

[b] Department of Naval Architecture, Ocean and Marine Engineering, University of Strathclyde, 100 Montrose Street, Glasgow, G4 0LZ, Scotland, UK

[c] Department of Naval Architecture, Technological Educational Institute of Athens, Egaleo, Greece

[1] These authors contributed equally to this work.

ABSTRACT

The continuous stringent requirements of the environmental regulations along with the LNG fuel penetration and the development of port and bunkering facilities, render the use of the dual fuel engines an attractive alternative of the traditional ship propulsion plants based on Diesel engines running with HFO for reducing both the plant operating cost and environmental footprint. The present study deals with the computational investigation of a large marine dual fuel (DF) engine of the four-stroke type for comparing its performance and emissions, in both diesel and gas mode operation by using the commercial software GT-ISE. The engine diesel model was initially set up and calibrated to adequately represent the engine operation. Subsequently, the engine dual fuel model was further developed by considering the injection of two different fuels; methane in the cylinder inlet ports and pilot diesel fuel into the engine cylinders. The derived results were analysed for revealing the differences of the engine performance and emissions at each operating mode. In addition, the turbocharger matching was investigated and discussed to enlighten the turbocharging system challenges due to the completely different air–fuel ratio requirements in diesel and gas modes, respectively. Finally, parametric simulations were performed for gas mode operation at different loads by varying pilot fuel injection timing, inlet valve closing and inlet manifold boost pressure, aiming to identify the engine settings that simultaneously reduce CO_2 and NOx emissions considering the air–fuel ratio operation window limitations. The parametric study results are discussed to infer the engine optimal settings.

Keywords: marine dual fuel four-stroke engines; low pressure gas injection, GT-ISE (GT-POWER) simulation; turbocharging system requirements; performance-emissions comparison; parametric investigation; engine optimal settings.

1 INTRODUCTION

Marine diesel engines gaseous emissions including CO_2, NOx, SOx, HC, CO and PM, have been steadily increasing throughout the last years. As it is reported in Bows–Larkin et al. (2014), shipping accounts for 2-3% of global gaseous emissions. For controlling gaseous emissions and air pollution as well as reducing the environmental impact of the maritime industry, various international and national regulatory bodies such as IMO, EMSA and EPA have adopted a series of regulations for limiting the non-greenhouse gaseous emissions including NOx and SOx, as well as the greenhouse gaseous emissions; mainly CO_2 as illustrated in IMO (2014), EMSA (2015) and EPA (2015).

Through these amendments of the international regulatory framework, the Energy Efficiency Design Index (EEDI) and the Energy Efficiency Operational Indicator (EEOI) were introduced. Based on the aforementioned, the Ship Energy Efficiency Management Plan (SEEMP) was established. The EEDI was made mandatory for newly built ships on 2013 whilst SEEMP for new and existing vessels on 2011 with the adoption of amendments to MARPOL Annex VI. The expected benefits from the implementation of the above include not only the reduction of the environmental impact of gaseous emissions, but also the reduction of the fuel consumption throughout the ship lifetime leading to minimised operating costs that affect the competitiveness of the shipping companies as it is discussed in Theotokatos & Tzelepis (2015). Furthermore, the price of LNG is also attractive; about 60% of the HFO price (Livanos et al., 2014), although the market is volatile and the fuels prices are affected by various parameters including geopolitical factors.

Responding to the imposed regulatory framework, the engine manufacturers e.g. MAN Diesel & Turbo (2012) and Wärtsilä (2015), as well as Classification societies e.g. ABS (2013) performed studies focusing on the gaseous emissions reduction (Jean-Michael, 2012), (Hendrik et al., 2016), (Bouman et al., 2017). In addition, the engine manufacturers have undergone efforts to improve the combustion characteristics, in order to improve the engines efficiency and consequently to reduce the associated fuel consumption, as well as to limit the engines gaseous emissions. Marine engine manufacturers have also developed dual fuel (DF) versions both for the large two-stoke slow speed engines and the small to medium size, four-stroke engines. These engines have the ability to operate on the gas and diesel modes; in the former by using natural gas and pilot diesel fuel, in the latter by burning diesel fuel (HFO or MGO).

As it is discussed in Livanos et al. (2014) and Abdelrahman et al. (2016), natural gas (NG) is the greenest fossil fuel that forms a well proven and feasible solution for ships propulsion. Whilst the conventional diesel fuels will remain the main preference for the majority of the existing vessels in the near future, the commercial opportunities of the natural gas are attractive for new-built vessels. The sulphur content of natural gas is almost zero (about 0.004% by mass), which is well below the 0.1% limit required for ECAs from 2015, and therefore the SOx emissions of the engines operating in gas mode are very limited (SOx emissions can be reduced up to 90-95% compared with the diesel mode operation at HFO). In addition, the DF four-stroke engines with low pressure admission can achieve up to 85% NOx emissions reduction as they operate in the lean burn combustion concept, the CO_2 emissions can decrease up to 20-25% due to the natural gas lower carbon to hydrogen ratio, whereas the particulate matter (PM) emissions are almost eliminated and there is no visible smoke during engine operation at gas mode.

There are two types of four-stroke engines differing in the gas injection; (a) the DF engines which operate at low gas pressure (5-7 bar) where the gas is injected at port and mixes with air during the intake phase (Wärtsilä, 2015) and (b) the gas-diesel (GD) engines which operate at high gas pressure (around 350 bar) where the gas is directly injected into the cylinder during the combustion phase. Both categories can achieve typical brake mean effective pressure (BMEP) of around 25 bar. Typical example of the first type is the Wärtsilä 50DF category whereas Wärtsilä 32 GD and 46 GD are classified under the second type (Jarf & Sutkowski, 2009). Likewise, there are two types of two-stroke DF engines classified by the gas injection and combustion processes concept; the first operates at high gas fuel pressure (around 300-350 bar) in which the gas fuel is injected during the combustion phase and is burnt according to the diffusive combustion concept as described in MAN Diesel & Turbo (2015), whereas the second operates in low gas fuel pressure (around 7 bar) in which the gas fuel is injected into the engine cylinder during the compression phase and burnt based on the premixed combustion concept as explained in Nylund et al. (2013).

Previous research efforts on dual fuel engines along with a review of the operation principles and practices are reported in Karim (2015). The research efforts reported in Krishnan et al. (2002), Cordiner et al. (2005), Kavtaradze et al. (2005), Srinivasan et al. (2006), Vasilev (2007), Ozcan et al. (2008), Papagianakis et al. (2010), Pirker et al. (2010), Jarvi (2010), Andre (2013), , Xu et al. (2014), Abagnale et al. (2014), Yousefi et al. (2015), Bo et al. (2015), Li (2016), Qiang et al. (2015), Zhongshu et al. (2015), Banck et al. (2016), Cameretti et al. (2016), Moriyoshi et al. (2016), Shinsuke et al. (2016), Wang et al. (2016), Georgescu et al. (2016) mainly dealt with the investigation of the dual fuel engines emission characteristics, the development of methods for increasing the DF engines efficiency, the optimisation of the pilot fuel injection and gas substitution rate, the extension of the operating range of gas mode and avoiding knocking. Simulation tools of various complexities (0D to 3D) (Singh et al., 2004), (Merker et al., 2006), (Coble et al., 2013), (Ritzke et al., 2016), (Theotokatos et al., 2016), (Mavrelos et. al., 2018) have been used for investigating the DF engine steady state performance and transient response (Xu et al., 2014), (Shuonan et. al., 2014). For analysing marine engines and ship propulsion systems, various model types have been also used as described in Benvenuto et al. (2013), Theotokatos & Tzelepis (2015), Baldi et al. (2015), Cichowicz et al. (2015) and Mizythras et al. (2018). However, very few studies have been published focusing on marine DF engines investigations. The control during fuel mode transition of a marine DF engine has been reported in Wang et al. (2015). Nylund (2007), Boeckhoff et al. (2010), Portin (2010), Mohr & Baufeld (2013), Mohand et al. (2013), Menghan et al. (2015), Weifeng et al. (2015) and Sixel et al. (2016) focused on experimental studies of marine DF engines reported providing details of the engine settings and operation, whereas a computational study of DF engine investigating the alternatives of turbocharging system, compression ratio and variable valve timing is reported in Christen & Brand (2013), where the DF engine combustion was modelled by considering the gas fuel only assuming limited contribution of the pilot fuel. Sixel et al. (2016) combined GT-Power with a developed combustion model and experiments to investigate a marine DF engine operating with either natural gas or menhanol.

In this respect, the main objective of the present study is to develop a model for a large marine dual-fuel engine of the four-stroke type, considering the engine processes and systems. Based on this, the investigation of the engine steady state performance and exhaust emissions is carried out at the engine discrete operating modes (diesel/gas). By analysing the derived results, the processes that affect the engine efficiency and gaseous emissions are revealed enabling the elaboration on possible ways to increase the engine efficiency and reduce emissions. In addition, the turbocharger matching along with the waste gate settings are discussed as different requirements are imposed in each operating mode. Finally, the optimisation of the engine settings at the gas mode is investigated based on a parametric study results and taking into account the CO_2 and NOx emissions reduction along with the engine operational limitations.

2 ENGINE MODELLING

2.1 *Investigated engine*

The Wärtsilä engine 9L50DF was used for the present study, which is a four-stroke, non-reversible, turbocharged and intercooled DF engine. The engine consists of nine cylinders placed in-line. This type of engine is widely used due to its high power output along with its fuel flexibility, low emission rates, high efficiency and reliability. The engine details are reported in the manufacturer project guide (Wärtsilä, 2015). The main engine characteristics are illustrated in Table 1. The engine layout and components are presented in Figure 1. As it is shown, a waste gate is used to by-pass a part of the exhaust gas from the turbocharger turbine in order to control the engine cylinders air–fuel ratio at the gas operating mode. Each engine cylinder includes a main fuel and a pilot fuel injector. Gas is injected by using solenoid valves at each cylinder inlet port (upstream the intake valves) during the engine induction process.

The engine operation at constant speed of 514 r/min was investigated in the present study. Engine operation under these conditions can be found in electric propulsion systems, where engine-electric generator sets are used for producing the ship required electric energy.

Table 1 Engine main characteristics

MCR power	kW	8775
MCR speed	r/min	514
BMEP at MCR	bar	20
BSFC at MCR (Diesel mode)	g/kWh	190
BSEC at MCR (gas mode)	kJ/kWh	7300
Bore	mm	500
Stroke	mm	580
No. of cylinders	-	9
Turbocharger units	-	1

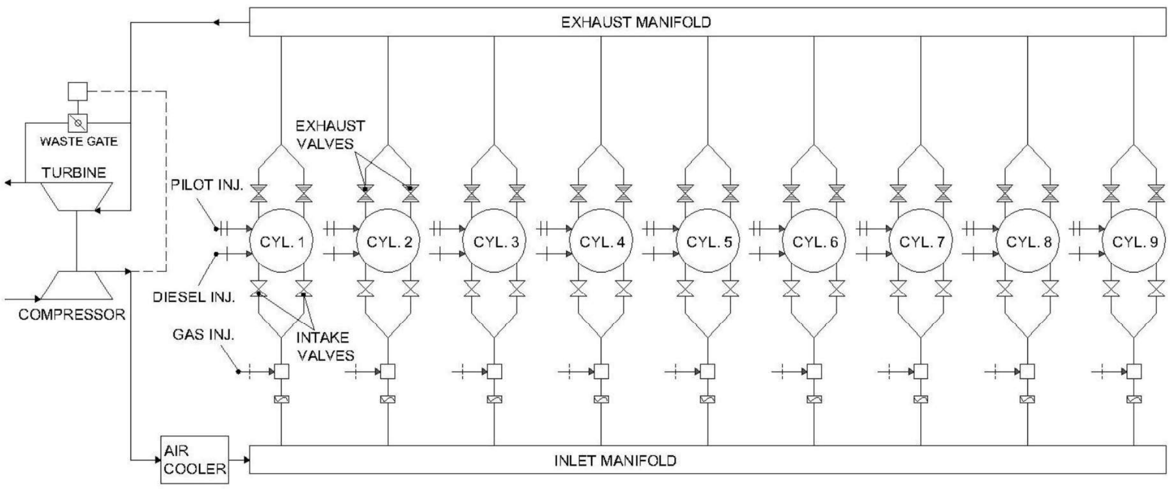

Figure 1 Engine layout

2.2 *Model set-up and calibration*

The software used in the present work is GT-ISE /GT-Power (Gamma Technologies, 2016), which is a widely used 1-D simulation program for engine modelling and analysis. GT-ISE is capable of, through a sophisticated set of solvers and algorithms, representing the physical processes within a working engine, to simulate the steady and transient states operation of various engine types. The main principle of the software is based on the ability of the user to build an accurate engine model in the software GUI, based on a broad range of items available in the software library. The software employs 1D gas dynamics to represent the flow in pipes, whereas 0D approach was used for the simulation of engine cylinders. Thus, it is able to predict the operating parameters of the engine and its components including pressures, mass flow rates and temperatures. The GT-ISE software is widely considered as one of the leading tools for these type of engine simulations due to its computational capabilities, results accuracy and fast execution time. In addition, the offered customisability and the coverage of a wide range of applications were considered advantageous characteristics for selecting the GT-ISE software in the present study.

The data required for the modelling stage as input was acquired from the product guide and the manufacturer engine 3D model presented in Wärtsilä (2015). Initially, the model for one-cylinder block was developed and validated for the diesel mode operation and subsequently, the model was extended to cover the dual fuel operation by adding an additional injector for the natural gas connected to the cylinder inlet port. Then the complete engine model including the turbocharger, waste gate and air cooler was developed as shown in Figure 2.

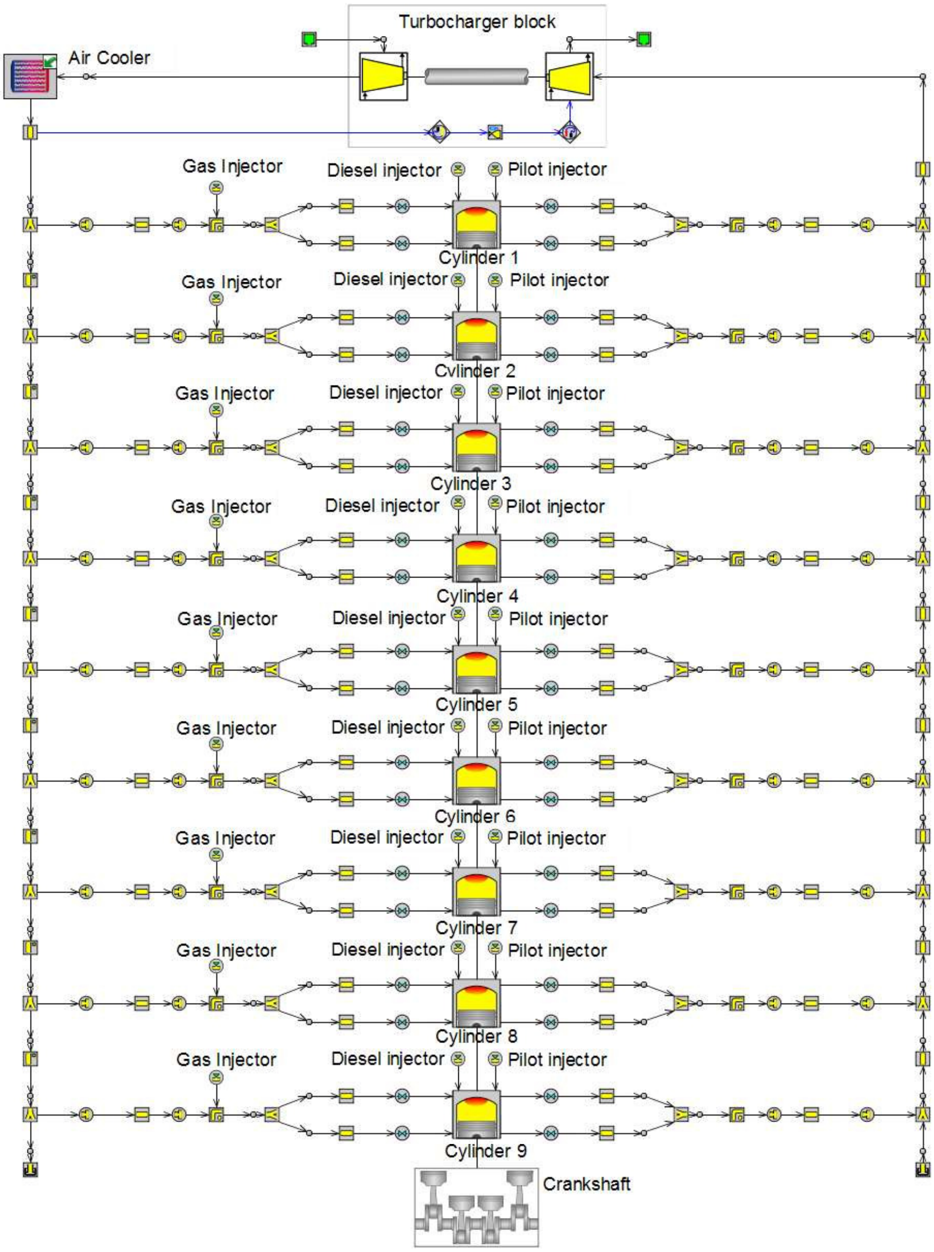

Figure 2 Engine model in the GT-ISE environment

The steps required to set up the engine model are as follows. Initially, the component blocks are selected, which sufficiently represent the engine layout and the appropriate interconnections are established. Then, the input data of all blocks are set. Preliminary calibration of the model constants is performed for a reference point and simulation runs are carried out. Finally, the fine tuning of the model constants is accomplished, so that the required accuracy is obtained.

The input data needed to set up the model includes the engine geometric data, the intake and exhaust valves profiles, the compressor and turbine performance maps, the waste gate geometric and control details, the constants of engine sub-models (combustion, heat transfer and friction), the engine operating point (load/speed) and the ambient conditions. Initial conditions are required for the temperature, pressure and composition of the working medium contained in the engine cylinders, pipes and receivers.

The Woschni heat transfer model initially presented in Woschni (1967) and extensively employed in various studies as described in Merker et al. (2006) was used to calculate the in-cylinder gas to wall heat transfer coefficient. The heat release rate was simulated according to single Wiebe model reported in Merker et al. (2006) for the engine diesel operating mode, whilst in the case of the gas mode, the multi-Wiebe model was utilised by imposing three different Wiebe curves corresponding to the premixed combustion of approximately half of the pilot fuel, the diffusive combustion of the remaining pilot fuel and the rapid burning of the gaseous fuel as well as the tail combustion of the cylinder residuals respectively. In this respect, the cumulative fuel burning rate for the gas mode is calculated according to the following equation (Gamma Technologies, 2016):

$$x_b(\theta) = \sum_{i=1}^{3}\left[\left(\frac{FF_i}{\sum_{i=1}^{3} FF_i}\right) x_{b,i}(\theta)\right] \qquad (1)$$

where FF denotes the fraction of fuel per Wiebe Curve; i denotes the Wiebe function; and θ denotes the crank angle (the 1st cylinder TDC at the closed cycle corresponds to 0 degrees CA).

The injection delay was estimated for the diesel mode according to the Sitkey equation as described in Merker et al. (2006), whereas the ignition delay for the gas mode was approximated by using the equations and data reported in Christen & Brand (2013) and Sixel et al. (2016).

For the simulation of the diesel mode operation, marine gas oil (MGO) was used as the considered fuel type along with the injection timing and injected fuel amount, which were provided as function of the engine load. For the gas mode, the amount of injected gaseous fuel per cycle (NG) was calculated by considering the known gas specific energy consumption and the fuel lower heating value. The gas fuel is injected at each cylinder intake port (upstream the inlet valves). The gas injection takes place during the respective cylinder induction process after the exhaust valve closing point, so that all the injected gas is inducted into the engine cylinders. The gas injection duration for each injector was considered to be a function of engine load taking values in the region from 38 to 68 degrees CA (from low to high loads), The engine valves timing was set according to the Miller timing concept in which the intake valves of each cylinder close before bottom dead centre (BDC). This reduces the required compression work and the combustion temperature resulting in higher engine efficiency and lower NOx emissions, however, high boost pressure and as a result, compressor pressure ratio values are needed.

For calculating NOx emissions, the Zeldovich model was used, which was calibrated only for 100% load operation at diesel and gas modes and subsequently was used to predict the NOx emissions at the other investigated loads. A two-zone cylinder model was employed considering a zone containing the combustion products and an unburned mixture zone. The temperature of the burned gas zone was used for estimating the NOx emissions. However, as the temperature spatial distribution was not calculated by the two-zone model, the NOx model is only capable of identifying trends and therefore, the derived results should be used with the necessary diligence.

Finally, the complete engine model with the air cooler, the turbocharger and waste gate was built for the diesel and gas modes. For the gas operating mode, the engine needs to operate within an air–fuel equivalence ratio in the range 2.0 to 2.3 for avoiding knocking and misfiring. This was achieved by controlling the waste gate valve to achieve a target value for boost pressure for each engine load. In GT-ISE, a PI controller was used to adjust the opening of the waste gate valve.

3 RESULTS AND DISCUSSION

The investigated marine DF engine steady state operation at both diesel and gas modes was examined by performing simulation runs in a load range from 25% to 100% and constant engine speed at 514 r/min. A set of the derived results including the cylinder maximum (peak) pressure, the indicated and brake mean effective pressures, the brake specific energy consumption, the brake efficiency, the turbocharger shaft speed, the boost pressure, the exhaust gas temperature before and after turbine along with their comparison to the respective available engine measured data from the engine shop trials is presented in Figure 3.The predicted engine parameters including the air and exhaust gas mass flow rates, the air–fuel equivalence ratio, the waste gate opening and the maximum temperature of the burned zone as well as specific NOx and CO_2 emissions are illustrated in Figure 4. The normalised cylinder pressure diagrams for the 100% load is shown in Figure 5, whereas the compressor operating points superimposed on the compressor map are presented in Figure 6. The percentage errors between the measured and predicted parameters are reported in Table 2.

From the plots presented in Figure 3 and the data given in Table 2, it is derived that the obtained accuracy was adequate (within the range of approximately ±3%). Therefore, it can be concluded that the developed model can be used to sufficiently represent the engine steady state behaviour.

Table 2 Percentage error between the measured and the predicted values

Diesel mode				
Load (%MCR)	P_b	p_{max}	T/C speed	Eff
100	2.60	0.16	0.04	-3.11
85	2.36	-0.60	-0.02	-2.90
75	1.88	0.19	-0.06	-2.43
50	1.14	0.42	-0.79	-1.64
25	1.22	1.77	0.02	-2.22
Gas mode				
Load (%MCR)	P_b	p_{max}	T/C speed	Eff
100	-0.42	0.37	0.75	2.49
85	-1.15	0.33	-0.32	3.43
75	-0.41	0.51	-0.90	2.32
50	1.70	0.42	-0.27	-1.16
25	1.34	0.60	1.14	-0.90

Table 3 Combustion model parameters for 100% load

Diesel mode				
Fuel	m	Δθ	SOC	Fraction
MGO	1.25	56	-3	1
Gas mode				
Fuel	m	Δθ	SOC	Fraction
Premixed combustion	1.5	15.3	-16.7	0.02
Main combustion	3	56.3	-16.7	0.96
Tail combustion	2	30.0	8.0	0.02

Wiebe parameter “a” equals to 6.9 for all curves

The combustion models parameters values (as used in equations (1) and (2)) calibrated to simulate the diesel and gas modes at 100% load are summarised in Table 3. By considering the derived pressure diagrams (Figure 5), it can be inferred that the diesel mode combustion starts closer to the cylinder top dead centre (TDC), whereas in the case of the gas mode the pilot injection and combustion starts earlier to avoid knocking problems. The gas mode operation also results in a longer ignition delay due to the natural gas presence in the combustion chamber as it is also reported in Liu & Karim (1997), Christen & Brand (2013) and Sixel et al. (2016). The peak heat release rate of the dual-fuel combustion is slightly higher and the main combustion ends earlier than that at the diesel mode. However, lower maximum pressure level is observed in the case of the gas mode, which is attributed to the engine turbocharger operation at lower speed due to the waste gate valve opening. As the boost pressure is lower in the case of the gas mode, the cylinder pressure during the compression process is also lower; however due to the advanced start of combustion and the shorter combustion duration, the lower maximum pressure and the resultant lower friction, the engine brake power is retained at the same level as in the diesel mode.

Therefore, in terms of the engine power output and mean effective pressures behaviour, it can be observed that similar values were obtained in each operating mode; the indicated mean effective pressure of the diesel mode seems to be only slightly greater, however the brake mean effective pressures in both modes are exactly the same as the difference is compensated by the slightly higher friction mean effective pressure (due to the greater maximum pressure of the diesel mode).

In terms of the air–fuel equivalence ratio (λ), it is observed from Figure 4 that in the gas mode the engine operates within a narrow λ window with values between 2.0 and 2.3 (2.3 was observed at the low loads whilst 2.0 was obtained at medium and high loads). For the diesel mode, the obtained values for λ are slightly higher (in the range from 2.5 to 2.9), which means that more air passes through the engine cylinders. For the gas operation, the waste gate opening affects (actually reduces) the turbocharger speed, which in turn controls the boost pressure and as a result, the engine air flow and λ. The obtained waste gate opening values were estimated in the range from 23% to 35% of the waste gate cross sectional area depending on the engine load.

As it can be seen in Figure 3 (turbocharger speed plot), figure 4 (mass flow rates plot) and figure 6 (compressor map), the turbocharger speed, pressure ratio and flow rate are considerably reduced in the gas mode when the engine operates at high loads. Smaller reductions can be observed at the lower loads (25% and 50%). This denotes that the turbocharger matching needs special attention for a DF engine compared to the respective process for diesel or gas engines, as in the former case, the requirements for the two discrete modes need to be satisfied. Especially for the compressor selection, a number of parameters (usually contradictory) have to be considered including targeting operation in the high efficiency area and providing adequate margins to avoid the compressor surging and the turbocharger overspeed.

In terms of the engine efficiency at the two operating modes, it can be observed that the gas mode is more efficient at the high loads region obtaining values up to 47% at 100% load. When operating in the diesel mode, the engine obtains its highest efficiency at 75% load, whereas the engine efficiency only slightly varies in the load region from 70% to 100%. For the gas mode, the efficiency decreases at a steeper gradient as the load decreases reaching its lowest value at 25% load; the engine obtains much higher efficiency at 25% load when operating at the diesel mode. This is attributed to the specific characteristics of diesel and gas operating modes as well as to the opening of the waste gate valve that results in lower turbocharger speed and pressure levels for the gas mode. Similar conclusions can be derived by analysing the brake specific energy consumption, which is the reciprocal of engine brake efficiency. The energy provided by the pilot diesel fuel accounts for 0.3% to 2.3% of the totally supplied fuel energy (the values increase with decreasing load).

Considering the calculated NOx and CO_2 emissions shown in Figure 4, the following remarks can be noted. The specific NOx emissions are lower for the case of the gas mode operation; the NOx emissions for the diesel mode comply with Tier II limits, whereas the Tier III limit requirements are satisfied for the gas mode. In addition, the lower specific NOx emissions value is obtained at 75% load whilst higher values of the specific NOx emissions are obtained at lower and higher loads. In the case of DF operation, NOx emissions slightly reduce at lower loads due to the premixed combustion of natural gas at greater values of air–fuel ratio.

The NOx differences between the engine operating modes can be explained by considering the in-cylinder burnt zone temperature plots (Figure 4) in conjunction with the cylinder pressure diagrams (Figure 5) and maximum cylinder pressure (Figure 3). As it can be inferred from these figures, at the diesel mode, the combustion occurs at greater pressure levels and the maximum temperature values of the burnt zone are greater than the respective values obtained for the gas mode; therefore higher NOx emissions are produced. On average, a reduction of 85% in NOx emissions is obtained when changing the operating mode from diesel to gas.

The CO_2 emissions of the gas mode are also reduced (by 25% in average) due to the lower carbon to hydrogen ratio of the natural gas compared to the respective one of diesel fuel. Larger reduction is obtained at the high loads region where the efficiency difference between the gas mode and diesel mode is greater. In summary, it can be concluded that the engine environmental impact is much lower when the engine operates at the gas mode.

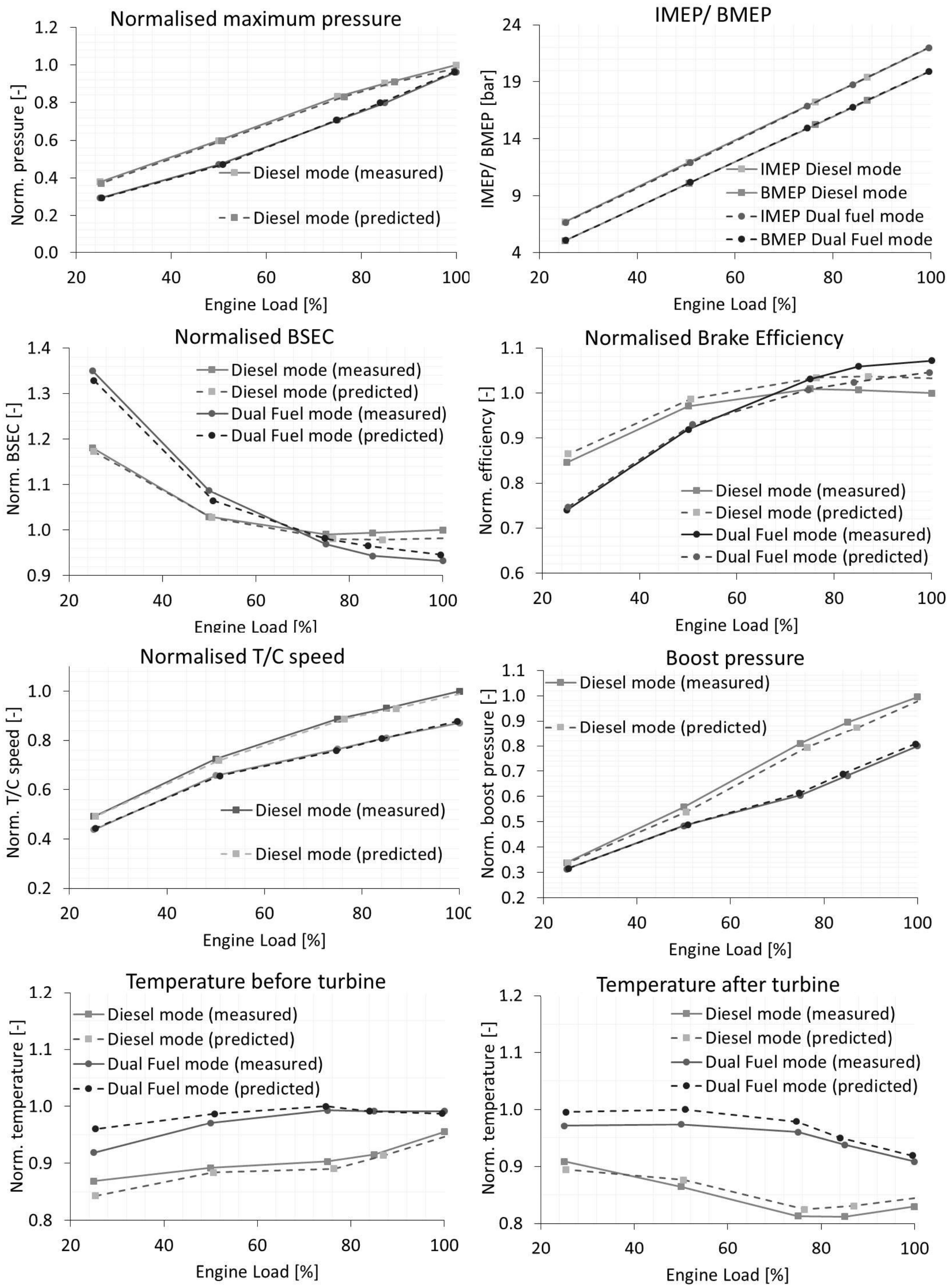

Figure 3 Simulation results and comparison with available experimental data. (The temperature plots were normalised by using the values in K; the pressure plots were normalised by using the pressure absolute values).

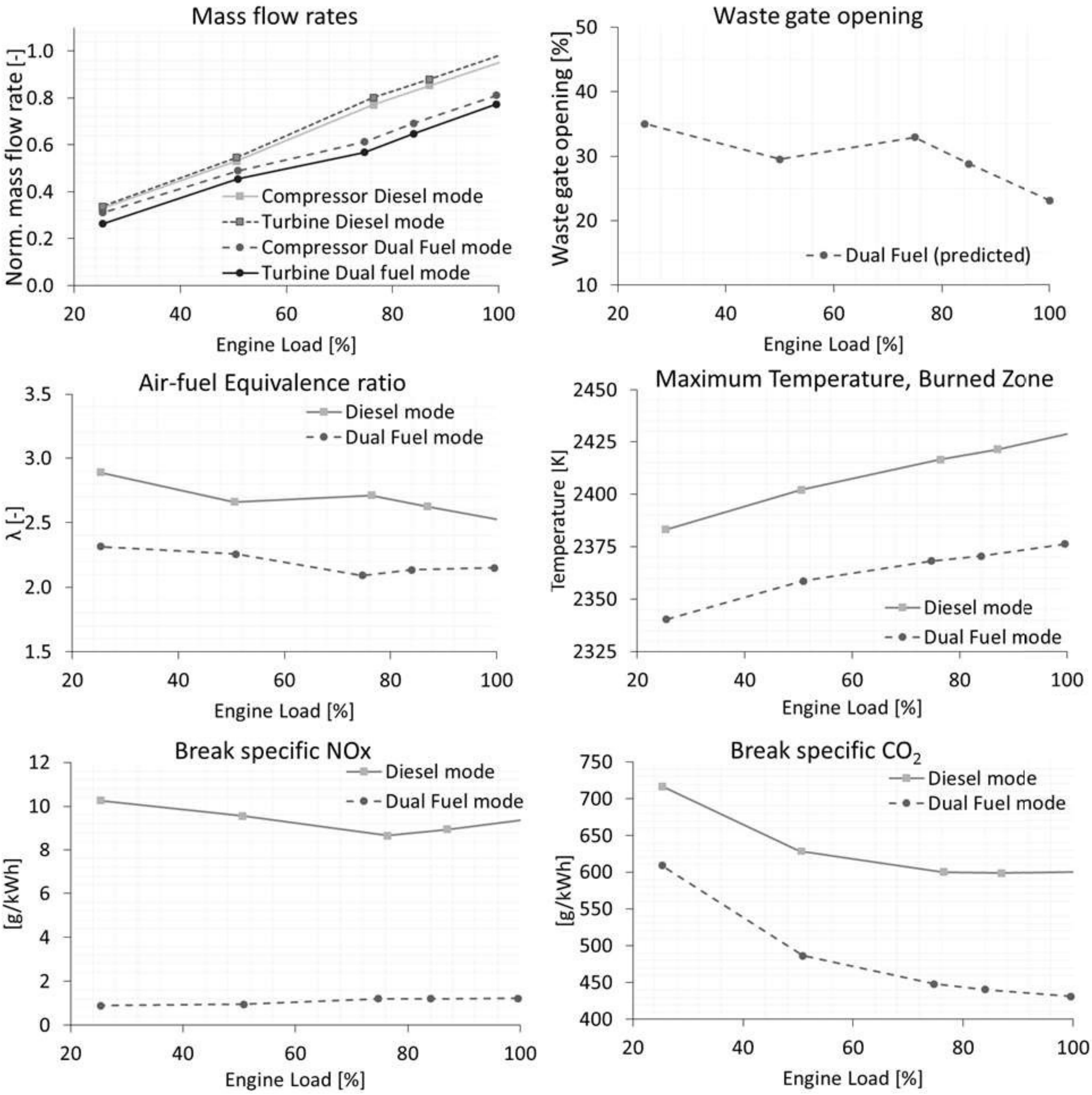

Figure 4 Predicted simulation results

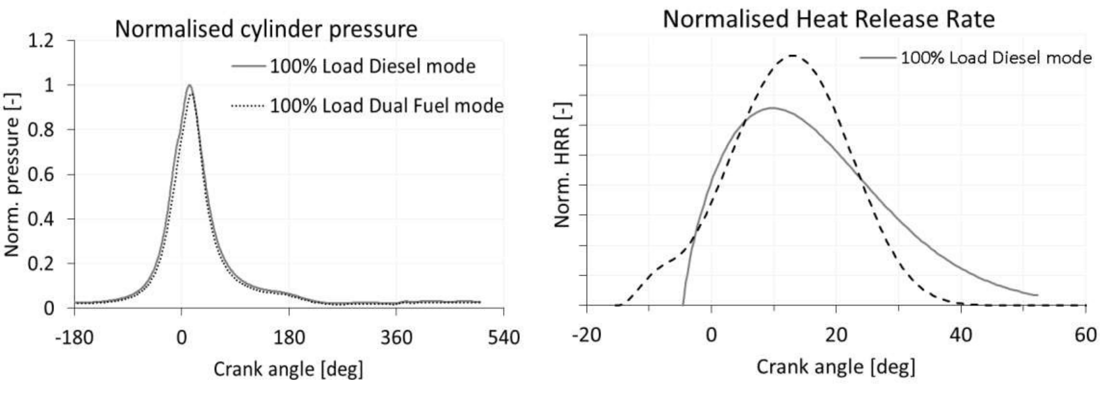

Figure 5 Pressure diagrams and heat release rates for diesel and dual fuel operation at 100% load

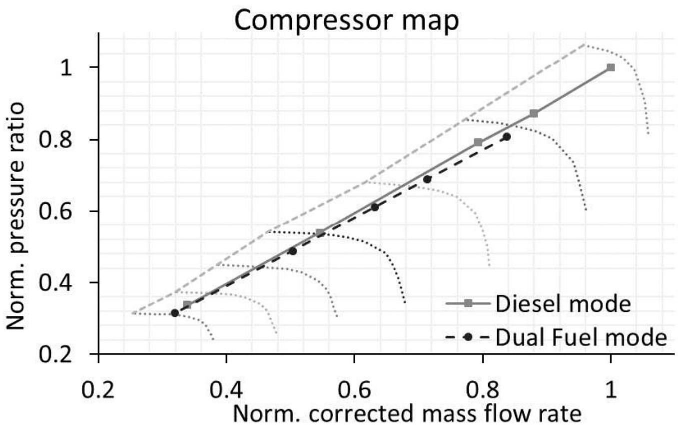

Figure 6 Compressor operating points superimposed on the compressor map for diesel and dual fuel operating modes

Having completed the engine model set up and the simulation of diesel and DF operating modes, a parametric study was performed for optimising the DF engine settings aiming to a simultaneous reduction of the CO_2 and NOx emissions. It must be noted that the CO_2 emissions are proportional to the engine specific energy consumption and therefore, a decrease of CO_2 emissions correspond to a reduction of BSEC and an increase of the engine brake efficiency. The following parameters were considered: pilot fuel injection timing (-2 and +2 degrees CA from the reference value), inlet manifold boost pressure (-5% and +5% from their reference value) and inlet valve closing (-5 and +5 degrees CA from the reference value). The results derived for 75% load along with the reference points (taken from the previously presented simulation results) are illustrated in Figure 7. It can be inferred from Figure 7 that the simultaneous reduction of CO_2 and NOx can be obtained by operating the engine in higher values of air–fuel equivalence ratio. However, the considered permissible lambda window from 1.9 to 2.3 (to avoid knocking and misfiring, respectively) resulted in the exclusion of a number of the performed parametric runs points. The used start of injection (at the reference point) provides a compromise between the CO_2 and the NOx emissions. Retarding the injection results in increased CO_2 emissions and reduced NOx emissions and vice versa. Therefore, the reference value for the start of injection was only considered for the parametric runs for 50% and 100% loads presented below. As indicated in the bottom plots of Figure 7, the engine operation with increased air–fuel equivalence ratio values can be achieved either by increasing the boost pressure (by closing the waste gate valve that results in higher exhaust gas mass flow through the turbine and therefore, increasing the turbocharger speed or retarding the inlet valve closing that results in more air trapped in the engine cylinder. A greater reduction potential for both CO_2 and NOx emissions is obtained by increasing the boost pressure as shown in the right-middle plot of Figure 7. The trade-off between the CO_2 and the NOx emissions as well as with the derived air–fuel equivalence ratio values are presented in Figure 8. By excluding the points outside the considered lambda window as well as the points with CO_2 and NOx emissions higher than the respective reference values, a limited number of points can be identified for a potential engine optimisation. The optimised point can be then selected based on the preferred optimisation criteria. In Table 4, the optimised points are provided for the following cases: a) maximum simultaneous reduction of the CO_2 and NOx emissions and b) maximum CO_2 emissions reduction and NOx emissions equal or less than the respective reference point value. For the former, point No 2 is the optimised point with 5% greater boost pressure, 5°CA inlet valve closing retard and no change in the pilot injection start, which results in reductions by 0.9% and 6.5% in the CO_2 and NOx emissions, respectively and an air–fuel equivalence ratio value equal to 2.21. Point No 3 having an additional pilot injection start advance of 2°CA (compared to point No 2) results in slightly greater air–fuel equivalence ratio (2.22) and reductions by 1.6% and 2.8% of the CO_2 and NOx emissions, respectively. If lower lambda values are needed, point No 1 can be considered with increased boost pressure by 5% compared to the reference point, resulting in lambda equal to 2.09 and reductions by 0.6% and 3.8% in the CO_2 and NOx emissions, respectively.

From the results presented in Figure 7 and Table 4 (the slopes of the respective curves), the relative significance of the three parameters used in the parametric runs can be identified. The inlet manifold boost pressure can be characterised as the main engine parameter for reducing both NOx and CO_2 emissions, whilst, the inlet valve closing can be considered of lower significance. The pilot fuel injection timing is also a parameter that considerably affects the emissions as shown in Figure 7, however, it exhibits a contradictory influence on the CO_2 and NOx emissions, as when the one increases, the other decreases and vice versa.

Furthermore, additional parametric runs were performed for 50% and 100% loads considering the reference point pilot start of injection and varying the boost pressure and the inlet valve closing. The derived CO_2-NOx emissions trade-off and the air–fuel equivalence ratio values are presented in

Figure 9. The permissible air–fuel equivalence ratio window for the case of 50% load was considered to be wider than the one of the 100% load case (from 1.5 to 2.3 versus 2.0 to 2.4, respectively) as indicated in Wärtsilä (2015). The green marks represent points with the same settings as the points 1 and 2 at 75% load. As it can be inferred from the analysis of Figure 9 results, there is potential for simultaneously reducing the CO_2 and NOx emissions. A greater reduction can be obtained in the NOx emissions (4.4 and 7.2% at 50% load 3.8 and 5.7% at 100% load), whereas the CO_2 emissions reduction is in the range of 0.7 to 0.8%. However, the resulting lambda values are considerably high (2.31 and 2.41) at 50% load, whereas the respective values are 2.17 and 2.28 at 100% load. Therefore, a boost pressure increase less than 5% might be used for the other load points to avoid misfiring, thus resulting in lower emissions reduction.

Another important parameter that needs to be considered in the engine optimisation study is the unburnt hydrocarbon emissions and in specific, the methane slip for the DF engines. This was not considered in this study as the 0D models cannot provide accurate results for the HC emissions, which apart from the thermodynamic and thermochemistry parameters are greatly influenced by the combustion chamber design. However, the parametric investigation study presented herein is quite useful in the preliminary stage of the engine design process as it provides insight information for the engine performance and emission parameters trade-offs.

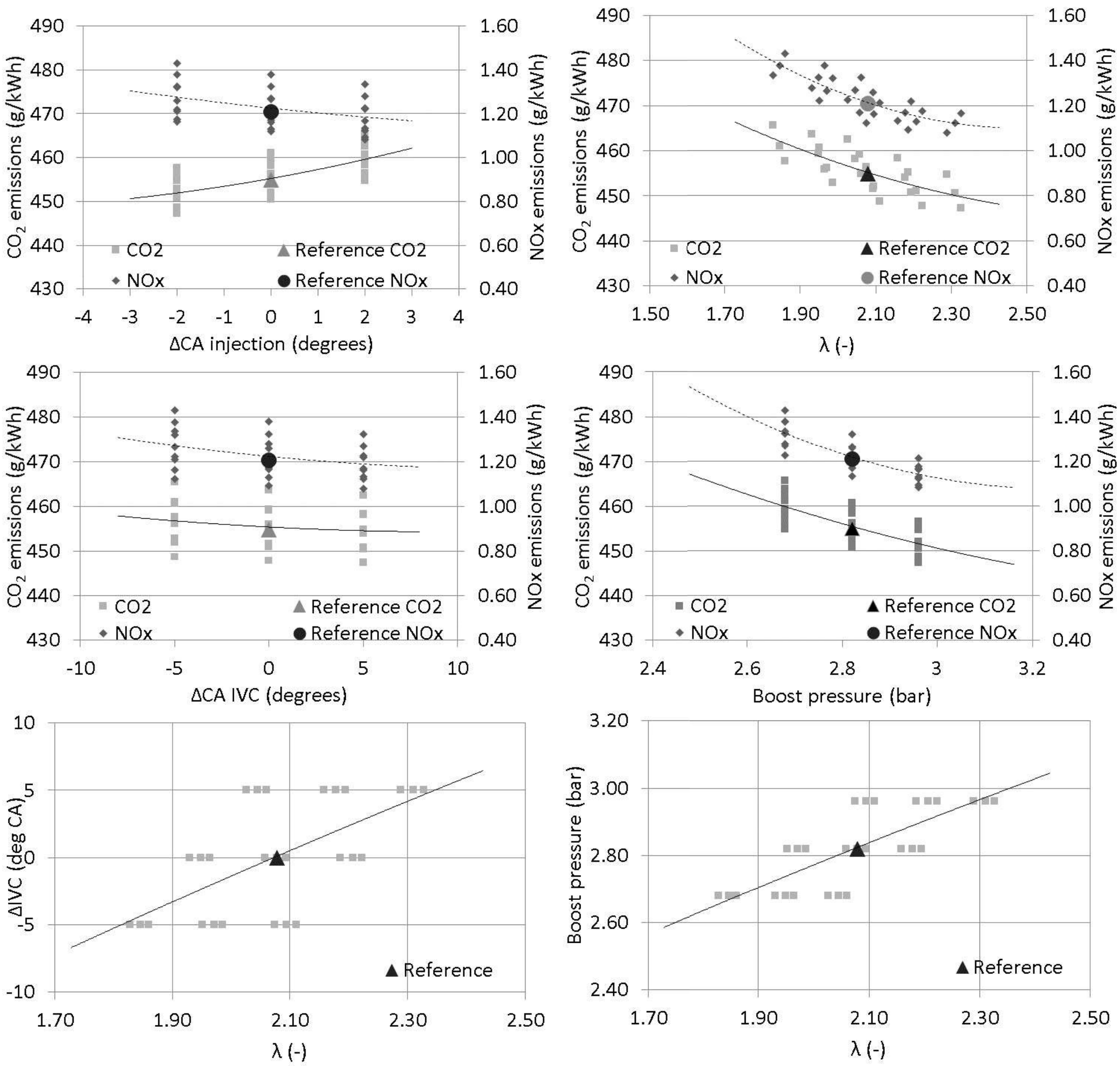

Figure 7 Parametric study results for DF engine operation at 75% load

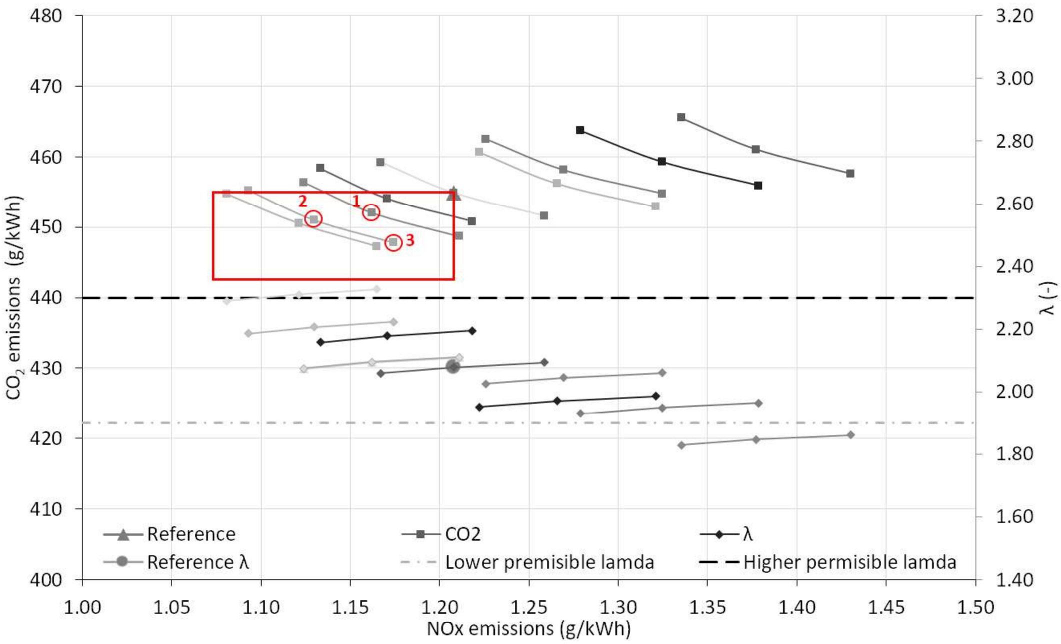

Figure 8 Parametric study results for DF engine operation at 75% load showing potential for CO_2 and NOx emissions reduction

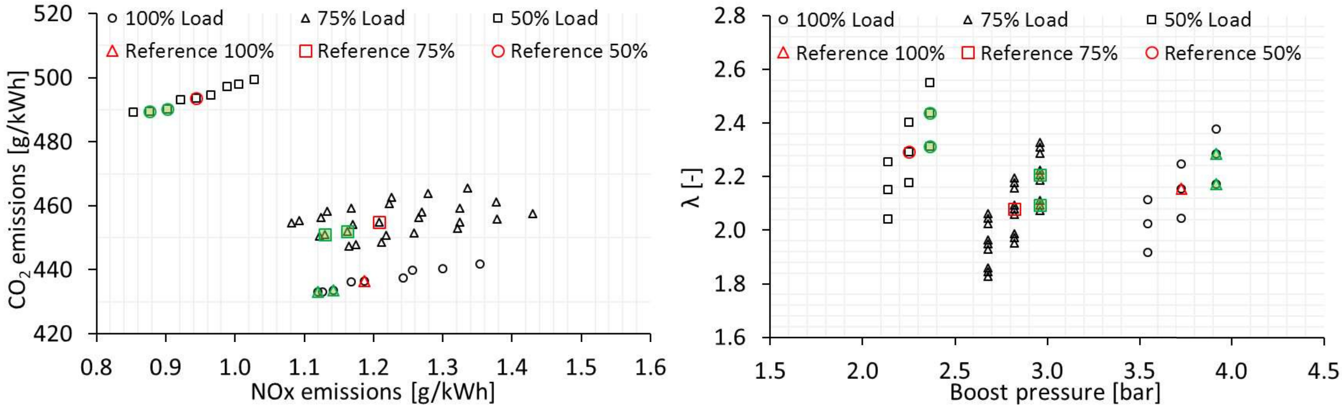

Figure 9 Parametric study results for DF engine operation at 50% and 100% load

Table 4 Optimised points from parametric runs

Load	No.	ΔIVC	ΔBoost pressure	ΔPilot Injection timing	Lamda	NOx	CO_2	ΔNOx	ΔCO_2
(%)	(-)	(ºCA)	(%)	(ºCA)	(-)	(g/kWh)	(g/kWh)	(%)	(%)
50%	-	0	5	0	2.31	0.9	490.3	-4.4	-0.7
	-	5	5	0	2.44	0.88	489.5	-7.2	-0.8
75%	1	0	5	0	2.09	1.16	452	-3.8	-0.6
	2	5	5	0	2.21	1.13	451	-6.5	-0.9
	3	5	5	-2	2.22	1.17	447.8	-2.8	-1.6
100%	-	0	5	0	2.17	1.14	433.6	-3.8	-0.7
	-	5	5	0	2.28	1.12	433	-5.7	-0.8

4 CONCLUSIONS

In the present study, a marine four-stroke dual fuel engine was investigated by using GT-ISE software in both diesel and gas mode operation. The engine performance and emissions parameters for both modes were compared and discussed. Parametric runs were performed and the results were used for deriving the engine setting that provide a simultaneous reduction of CO_2 and NOx emissions considering the engine operating limitations. The main findings of the conducted research are summarised as follows:

- The developed model can predict with adequate accuracy the engine performance and emissions parameters both for the diesel and DF operation and can be used in the preliminary stage of the engine design process for optimising the engine settings.
- The engine in the gas mode operates with almost constant air–fuel equivalence ratio in a narrow window from 2.0 to 2.3, whereas slightly higher values of the air–fuel equivalence ratio are used for the diesel mode corresponding to greater air flow rates. This is obtained by controlling waste gate valve opening (for gas mode) to adjust the engine air flow and therefore the air–fuel ratio. Special attention must be paid during the turbocharger matching process as there are different requirements in each operating mode including avoidance of turbocharger overspeed, providing an adequate compressor surge margin and operating the compressor within its high efficiency area.
- In the gas mode, the engine operates at lower receivers and in-cylinder pressure level. However, the mean effective pressure and power output is kept at the diesel mode levels due to the shorter combustion duration and the earlier start of combustion.
- The gas mode is more efficient than diesel mode at the high load region; however, less efficient operation was observed at the lower load region.
- The NOx emissions reduced by 85% in average in the gas mode compared with the diesel mode. The diesel mode complies with the Tier II limits, whereas Tier III limits are met when the engine operated in the gas mode.
- Increasing the engine boost pressure and/or retarding the Miller timing inlet valve closing can result in NOx and CO_2 emissions reduction.

- Compared to the reference point settings, the engine NOx and CO_2 emissions can be reduced up to 6% and 1.6%, respectively by increasing the inlet boost pressure by 5% and/or by retarding the Miller timing inlet valve closing by 5 degrees CA. However, limitations apply due to air–fuel ratio operation window and the potential hydrocarbon emissions (methane slip) increase.
- The derived results verify that the CO_2 emissions in the gas mode reduced approximately 25% in average due to the natural gas low carbon to hydrogen ratio. Larger reduction is obtained when the engine operates at the high load region where the efficiency is greater than that of the diesel mode.

In conclusion, it can be stated that the utilisation of natural gas, which can be stored and handled in liquefied phase (LNG) can provide an attractive and environmentally friendly alternative that should be considered and adopted in the future ship designs. The obtained results can be used as guidance during the design process of the dual fuel engines or when designing a vessel energy management system.

NOMENCLATURE

Eff	Brake efficiency (-)
FF	Fuel fraction per Wiebe Curve (-)
P_b	Brake power (kW)
p_{max}	Maximum cylinder pressure (bar)
$x_b(\theta)m$	Burning rate as a function of crank angle
ΔIVC	Inlet valve closing difference
$\Delta\theta$	Combustion duration (deg CA)
θ	Crank angle (0=TDC)
λ	Air–fuel equivalence ratio (-)
τ	Normalised time used in Wiebe function (-)

ABBREVIATIONS

0D	Zero-dimensional
1D	One-dimensional
3D	Three-dimensional
BMEP	Brake Mean Effective Pressure
BSEC	Brake Specific Energy Consumption
BSFC	Brake Specific Fuel Consumption
CA	crank angle
CO	Carbon Monoxide
CO_2	Carbon Dioxide
DF	Dual Fuel
ECA	Emission Control Area
ECU	Engine Control Unit
EEDI	Energy Efficiency Design Index
EEOI	Energy Efficiency Operational Indicator
HC	Hydrocarbons
HFO	Heavy Fuel Oil
IMO	International Maritime Organization
LNG	Liquefied Natural Gas
MARPOL	International Convention for the Prevention of Marine Pollution
MCR	Maximum continuous rating
MGO	Marine Gas Oil
NG	Natural Gas
NOx	Nitrogen Oxides
PM	Particular Matter
SEEMP	Ship Energy Efficiency Management Plan
SOC	Start of combustion
SOx	Sulphur Oxides
TDC	Top Dead Centre
T/C	Turbocharger

AKNOWLEDGMENTS

Gamma Technologies support is greatly acknowledged by the authors.

REFERENCES

Abagnale, C., Cameretti, M., De Simio, L., M., G., Iannaccone, S., & Tuccillo, R. (2014). Numerical simulation and experimental test of dual fuel operated diesel engines. *Applied Thermal Engineering*, 403-417. doi:http://dx.doi.org/10.1016/j.applthermaleng.2014.01.040

Abdelrahman, H., Antonino, L. R., & Paul, S. (2016). Towards keeping diesel fuel supply and demand in balance: Dual-fuelling of diesel engines with natural gas. *Renewable and Sustainable Energy Reviews*. doi:http://dx.doi.org/10.1016/j.rser.2016.11.249

ABS. (2013). Ship Energy Efficiency Measures - Status and Guidance. *Publication No. TX 05/13 5000 13015.*

Amit, B., Markus, K., Luca, M., & Fabian, M. (2004). Modelling a Dual-fuelled Multi-cylinder HCCI Engine Using a PDF based Engine Cycle Simulator. *SAE*.

Andre, R. (2013). Dual-Fuel for maritime application. In Proceedings of the 27th CIMAC World Congress on Combustion Engine Technology, Shanghai, China, 13–16 May 2013; Paper no. 204.

Ashok, B., Denis, S., Ashok, C., & Ramesh, K. (2015, April 1). LPG diesel dual fuel engine – A critical review. *Alexandria Engineering Journal*. doi:http://dx.doi.org/10.1016/j.aej.2015.03.002

Baldi, F., Theotokatos, G., & Andersson, K. (2015). Development of a combined mean value zero dimensional model and application for a large marine four-stroke Diesel engine simulation. *Applied Energy. 154; 402-415.*

Banck A., Eike, S., & Carsten, R. (2016). Dual Fuel Engine optimized for marine applications. *28th CIMAC World Congress 2016* (p. 047). Helsinki: CIMAC.

Benvenuto, G., Campora, U., & Laviola, M. (2013). Simulation Model of a Methane-Fuelled Four Stroke Marine Engine for Studies on Low Emission Propulsion Systems. *IMAM 2013, 15th International Congress on Maritime Association of the Mediterranean* (pp. Pages 591–597). Acorugna, Spain: CRC Press 2013. doi:10.1201/b15813-72

Bo, Y., Chengxun, X., Xing, W., Ke, Z., & Ming-Chia, L. (2015). Parametric investigation of natural gas port injection and diesel pilot injection on the combustion and emissions of a turbocharged common rail dual-fuel engine at low load. *Applied Energy*, 130–137. doi:http://dx.doi.org/10.1016/j.apenergy.2015.01.037

Boeckhoff, N., Heider, G., & Hagl, P. (2010). Operational experience of the 51/60 DF from MAN Diesel SE, PAPER NO.: 37. *CIMAC*. Bergen.

Bows–Larkin, Mander, A., Gilbert, S., Traut, P., & Walsh, M. (2014). *High Seas, High Stakes, High Seas Final Report.* University of Manchester, School of Mechanical Aerospace and Civil Engineering. Tyndall Centre for Climate Change Research. Retrieved from http://www.lowcarbonshipping.co.uk/files/ucl_admin/High_Seas_High_Stakes_High_Seas_Project_Final_Report.pdf

Cameretti, M., Tuccillo, R., De Simio, L., Iannaccone, S., & Ciaravola, U. (2016). A numerical and experimental study of dual fuel diesel engine for different injection timings. *Applied Thermal Engineering*, 630–638. doi:http://dx.doi.org/10.1016/j.applthermaleng.2015.12.071

Christen, C. and Brand, D. (2013). IMO Tier 3: Gas and dual fuel engines as a clean and efficient solution. Paper no. 187. 27th CIMAC World Congress on Combustion Engine Technology, Shanghai, China, 13–16 May 2013.

Cichowicz, J., Theotokatos, G., & Vassalos, D. (2015). Dynamic energy modelling for ship life-cycle performance assessment. Ocean Engineering, 110, 49-61.

CIMAC (2012). EMISSION CALCULATION CHECK GUIDE – IMO NOx Technical Code 2008. The International Council on Combustion Engines, Working Group 'Exhaust Emissions Control' Members. http://www.cimac.com/cms/upload/workinggroups/WG5/CIMAC_Exhaust_Emissions_Control_Quality_Guide_IMO_NOx_Technical_Code_2008_FINAL.pdf [Accessed 23 Dec 2017].

CIMAC. (2011). *TRANSIENT RESPONSE BEHAVIOUR.* CIMAC WORKING GROUP “GAS ENGINES”. Frankfurt: CIMAC.

Ciulli, E. (1993). A review of internal combustion engine losses, pt. 2: studies for global evaluations. Proceedings of the Institution of Mechanical Engineers, Part D: Journal of Automobile Engineering, 207(3), pp.229-240.

Coble, A., Smallbone, A., Bhave, A., Mosbach, S., Kraft, M., Niven, P. and Amphlett, S. (2011). Implementing Detailed Chemistry and In-Cylinder Stratification into 0/1-D IC Engine Cycle Simulation Tools. SAE Technical Paper Series 2011-01-0849. doi:10.4271/2011-01-0849.

Cordiner, S., Rocco, V., Scarcelli, R., Gambino, M., Iannaccone, s., & Setaro, G. (2005). Numerical and Experimental Analysis of the Behaviour of a Heavy-Duty Diesel Engine Converted to Dual-Fuel Operations. *SAE Technical Paper 2005-24-032*. doi:10.4271/2005-24-032

EMSA. (2015). *emsa.europa.eu*. Retrieved from em-sa.europa.eu/main/air-pollution.html.

EPA. (2010). Control of Emissions from New Marine Compression-Ignition Engines at or Above 30 Liters per Cylinder; Final Rule. Federal Register/Rules and Regulations. 75(83), 30 April 2010.

EPA. (2015). *www.epa.gov*. Retrieved from www.epa.gov/otaq/marine.htm.

Bouman E., Lindstad E., Rialland A., Strømman A. (2017). State-of-the-art technologies, measures, and potential forreducing GHG emissions from shipping – A review. *Transportation Research Part D*, 408–421. doi:http://dx.doi.org/10.1016/j.trd.2017.03.022

Gamma Technologies. (2016). *GT Reference Manual.*

Georgescu, I., Douwe, S., & Benny, M. (2016). Dynamic Behaviour of Gas and Dual-Fuel Engines: Using Models and Simulations to Aid System Integration, PAPER NO.: 126. *28th CIMAC World Congress 2016.* Helsinki.

Hendrik, L., Andreas, B., & Eike, S. (2016). Investigation of alternative dual fuel engine concepts. *28th CIMAC World Congress 2016* (p. 212). Helsinki.

Heywood, J. B. (1998). *Internal combustion engine fundamentals.* Mc-Graw-Hill, Inc.

Hoenders R. (2013). EU Initiatives regarding the use of LNG as bunker fuel and EMSA’s involvement in promoting the use of LNG as alternative fuel. European Maritime Safety Agency (EMSA). July 2013.

IMO. (2014). MARPOL Annex VI, Regulation 13.

IMO. (2014). MARPOL Annex VI, Regulation 14.

Jarf, C., & Sutkowski, M. (2009). *The Wärtsilä 32GD engine for heavy gases*. (Wärtsilä) Retrieved January 2018, from Polish Scientific Society of Combustion Engines: http://www.combustion-engines.eu/en/numbers/36/147

Jarvi, A. (2010). Methane slip reduction in Wartsila lean burn gas, PAPER NO.: 106. 26th CIMAC World Congress 2010. Bergen, Norway.

Jean-Michael H. (2012). Retrofit of Wärtsilä diesel engine to Dual fuel. *Colloque optimisation énergétique des navires.* Marseille.

Karim, G. (March 2, 2015). *Dual-Fuel engines.* CRC Press, Taylor & Francis Group.

Kavtaradze, R. Z., Zeilinger, K., & Zitzler, G. (2005). Ignition Delay in a Diesel Engine Utilizing Different Fuels. *High Temperature, 43*(6), 947–956.

Krishnan, S. R. (2002). Performance and heat release analysis of a pilot-ignited natural gas engine. *International Journal of Engine Research, 3(3), 171-184.*

Kyriakides, N., Chryssakis, C. and Kaiktsis, L. (2009). Influence of Heavy Fuel Properties on Spray Atomization for Marine Diesel Engine Applications. SAE Technical Paper Series.

Li, Y. (2016). Research on the Influence of Diesel Injection Law to Combustion Process of Micro Ignition Dual Fuel Engine, PAPER NO.: 306. *28th CIMAC World Congress 2016.* Helsinki.

Liu, Z., & Karim, G. (1997). Simulation of combustion pro-cesses in gas-fuelled diesel engines. *Proceedings of the Institution of Mechanical Engineers, Part A: Journal of Power and Energy, 211(2):159-169/1997.*

Livanos, G., Theotokatos, G., & Pagonis, D. (2014). Techno-economic investigation of alternative propulsion plants for ferries and roro ships. *Energy Conversion and Management*, (pp. 79:640-651). doi:10.1016/j.enconman.2013.12.05

MAN Diesel & Turbo. (2012). SFOC Optimization Methods for MAN B&W Two-Stroke IMO Tier II Engines,. *MAN Diesel & Turbo: Augsburg, Germany; Publication no. 5510-0099-00ppr.*

MAN Diesel & Turbo. (2015). ME-GI Gas-ready Ship. *MAN Diesel & Turbo. Publication No. 5510-0176-00ppr, Aug 2015, Denmark*.

Mavrelos, C., & Theotokatos, G. (2018). Numerical Investigation of a Premixed Combustion Large Marine Two-Stroke Dual Fuel Engine for Optimising Engine Settings via Parametric Runs. *Energy Conversion and Management*.

Menghan, L., Qiang, Z., Guoxiang, L., & S. S. (2015). Experimental investigation on performance and heat release analysis of a pilot ignited direct injection natural gas engine. *Energy*, 1-10. doi:http://dx.doi.org/10.1016/j.energy.2015.06.089

Merker, G., Schwarz, C., Stiesch, G., & Otto, F. (2006). Simulating Combustion. Berlin, Germany: Springer-Verlag.

Mizythras P, Boulougouris E, Theotokatos G. (2018) Numerical study of propulsion system performance during ship acceleration, Ocean Engineering. 10.1016/j.oceaneng.2017.12.010

Mohand Said, L., Khaled, L., Lyes, T., & Mourad, B. (2013). Towards improvement of natural gas-diesel dual fuel mode: An experimental investigation on performance and exhaust emissions. Energy, 200-211. doi:http://dx.doi.org/10.1016/j.energy.2013.10.091

Mohr, H., & Baufeld, T. (2013). Improvement of dual-fuel-engine technology for current and future applications, PAPER NO.: 412. *CIMAC.* Shanghai.

Moriyoshi, Y., Xiong, Q., Kuboyama, T. and Morikawa, K. (2016). Combustion Analysis in a Natural Gas Engine with Pre-Chamber to Improve Thermal Efficiency. In Proceedings of the 28th CIMAC World Congress on Combustion Engine Technology, Helsinki, Finland, 6–10 June 2016

Nylund I., & Ott, M. (2013). Development of a Dual Fuel technology for slow-speed engines, Paper No. 284. 27th CIMAC World Congress 2013. Shanghai, China.

Nylund, I. (2007). Field expirience with the Wärtsilä 50DF Dual fuel engine, PAPER NO.: 239. *CIMAC.* Vienna.

Ozcan, H., & Yamin, J. (2008). Performance and emission characteristics of LPG powered four stroke SI engine under variable stroke length and compression ratio. Energy Conversion and Management, 49(5), 1193-1201. http://dx.doi.org/10.1016/j.enconman.2007.09.004

Papagianakis, R., Rakopoulos, C., Hountalas, D., & Rakopoulos, D. (2010). Emmision characteristics of high speed, dual fuel, compression ignition engine operating in a wide range of natural gas/diesel fuel proportions. *FUEL - 17th International Symposium on Alcohol Fuels, 89*, 1397–1406. doi:10.1016/j.fuel.2009.11.001

Pirker, G., Losonczi, B., Fimml, W., Wimmer, A. and Chmela, F. (2010). Predictive Simulation of Combustion and Emissions in Large Diesel Engines with Multiple Fuel Injection. In Proceedings of the 26th CIMAC World Congress on Combustion Engine Technology, Bergen, Norway, 14–17 June 2010; Paper no. 235.

Portin, K. (2010). Wärtsilä dual fuel (DF) enines for offshore applications and mechanical drive, PAPER NO.: 112. *CIMAC.* Bergen.

Qiang, Z., Na, L., & Menghan, L. (2015). Combustion and emission characteristics of an electronically-controlled common-rail dual-fuel engine. *Journal of the Energy Institute*, 766-781. doi:http://dx.doi.org/10.1016/j.joei.2015.03.012

Ritzke, J., Andree, S., Theile, M., Henke, B., Schleef, K., Nocke, J. and Hassel, E. (2016). Simulation of a Dual-Fuel Large Marine Engines using combined 0/1-D and 3-D Approaches. In: The International Council on Combustion Engines. In Proceedings of the 28th CIMAC World Congress on Combustion Engine Technology, Helsinki, Finland, 6–10 June 2016; Paper no. 213.

Savva, N. and Hountalas, D. (2014). Evolution and application of a pseudo-multi-zone model for the prediction of NOx emissions from large-scale diesel engines at various operating conditions. Energy Conversion and Management, 85, pp.373–388.

Shinsuke, M., Thomas, K., Robert, S., Michael, Z., Ingo, K., & Andrei, L. (2016). Holistic Approach for Performance and Emission Development of High Speed Gas and Dual Fuel Engines. *28th CIMAC World Congress 2016* (p. 273). Helsinki.

Shuonan, X., David, A., Amrit, S., & Mark, H. (2014). Development of a Phenomenological Dual-Fuel Natural Gas Diesel Engine Simulation and Its Use for Analysis of Transient Operations. *SAE*. doi:10.4271/2014-01-2546

Singh, S., Kong, S., Reitz, R., Krishnan, S., & al., e. (2004). Modelling and Experiments of Dual-Fuel Engine Combustion and Emissions. *SAE Technical Paper 2004-01-0092*. doi:10.4271/2004-01-0092

Sixel, E. J., Hiltner J., & Rickert C. (2016). Use of 1-D simulation tools with a physical combustion model for the development of Diesel-Gas or Dual Fuel engines, PAPER NO.: 124. *28th CIMAC World Congress 2016*. Helsinki.

Srinivasan, K., Krishnan, S., & Midkiff, K. (2006). Improving low load combustion, stability and emissions in pilot-ignited natural gas engines. *Proceedings of the Institution of Mechanical Engineers, Part D: Journal of Automobile Engineering*, *220*, pp. 229-239. doi:10.1243/09544070JAUTO104

Theotokatos, G., & Tzelepis, V. (2015). A Computational study on the performance and emissions parameters mapping of a ship propulsion system. *Proc. IMechE Part M: J. Eng. Mar. Environ. 229, 58–76.*

Theotokatos, G., Stoumpos, S., Lazakis, I., & Livanos, G. (2016). Numerical study of a marine dual-fuel four-stroke engine. In C. G. Soares, & T. A. Santos (Eds.), Maritime Technology and Engineering III: Proceedings of the 3rd International Conference on Maritime Technology and Engineering (MARTECH 2016, Lisbon, Portugal, 4-6 July 2016). (Vol. 2, pp. 777-783). London. DOI: 10.1201/b21890-100

Vasil'ev, A. (2007). Ignition Delay in Multifuel Mixtures. *Combustion, Explosion, and Shock Waves, 43*(3), 282–285.

Wang, B., Li, T., Ge, L., & Ogawa, H. (2016). Optimization of combustion chamber geometry for natural gas engines with diesel micro-pilot-induced ignition. Energy Conversion and Management, 122, 552-563. http://dx.doi.org/10.1016/j.enconman.2016.06.027

Wang, H., Kolmanovsky, I., Sun, J., & Ozaki, Y. (2015). Feedback control during mode transition for a marine dual fuel engine. International Federation of Automatic Control (IFAC) Papers on Line, 279–284. doi:10.1016/j.ifacol.2015.10.293

Wärtsilä. (2015). Improving engine fuel and operational efficiency. *Wärtsilä services business white paper engine fuel and operational efficiency.* Retrieved from http://cdn.wartsila.com/docs/default-source/services-documents/white-papers/wartsila-bwp-improving-engine-fuel-and-operational-efficiency-2015.pdf?sfvrsn=6

Wärtsilä. (2015). *Product Guide Wärtsilä 50DF.* Wärtsilä. Retrieved from http://www.wartsila.com/products/marine-oil-gas/engines-generating-sets/dual-fuel-engines/wartsila-50df: http://www.wartsila.com/products/marine-oil-gas/engines-generating-sets/dual-fuel-engines/wartsila-50df

Wei, H., Chen, X., Wang, G., Zhou, L., An, S. and Shu, G. (2017). Effect of swirl flow on spray and combustion characteristics with heavy fuel oil under two-stroke marine engine relevant conditions. Applied Thermal Engineering, 124, pp.302-314. https://doi.org/10.1016/j.applthermaleng.2017.05.202

Weifeng, L., Zhongchang, L., & Zhongshu, W. (2015). Experimental and theoretical analysis of the combustion process at low loads of a diesel natural gas dual-fuel engine. Energy, 728-741. doi:http://dx.doi.org/10.1016/j.energy.2015.11.052

Woschni, G. (1967). A Universally Applicable Equation for the Instantaneous Heat Transfer Coefficient in the Internal Combustion Engine (Vol. 76). *SAE Technical Paper 670931.* doi:10.4271/670931

Xu, S., Anderson, D., Singh, A., Hoffman, M., Prucka, R., & Filipi., Z. (2014). Development of a Phenomenological Dual-Fuel Natural Gas Diesel Engine Simulation and Its Use for Analysis of Transient Operations. *SAE Int. J. Engines. 7(4). 1665-1673.*

Yang, L., Song, E., Ding, S., Brown, R., Marwan, N. and Ma, X. (2016). Analysis of the dynamic characteristics of combustion instabilities in a pre-mixed lean-burn natural gas engine. Applied Energy, 183, pp.746-759.

Yousefi, A., Birouk, M., Lawler, B., & Gharehghani, A. (2015). Performance and emissions of a dual-fuel pilot diesel ignition engine. *Energy Convietion Management, Paper No. JERT-16-1051.* doi:10.1115/1.4033707

Zhongshu, W., Zhongxiang, Z., Dan, W., Manzhi, T., Yongqiang, H., & Zhongchang, L. (2015). Impact of pilot diesel ignition mode on combustion and emissions characteristics of a diesel/natural gas dual fuel heavy-duty engine. Fuel, 248–256. doi:http://dx.doi.org/10.1016/j.fuel.2015.11.077